

Prehistory probability distribution of ionic transitions through a graphene nanopore[¶]

C. Guardiani*, M.L. Barabash*, W.A.T. Gibby*, D.G. Luchinsky*[†] I.A. Khovanov[‡] and P.V.E. McClintock*

*Department of Physics

Lancaster University, Lancaster, UK, LA1 4YB

Email:c.guardiani@lancaster.ac.uk

[†]SGT Inc., Ames Research Center, Moffet Field, CA, 94035, USA

[‡]School of Engineering University of Warwick, Coventry, CV4 7AL, UK

Abstract—We analyze selective ionic conduction through an artificial nanopore in a single graphene sheet, using molecular dynamics simulations and the prehistory probability distribution. We assess position-dependent changes in the number and orientation of water molecules in the first and second hydration shells of the ion as it crosses the nanopore. We reveal coupling between an ionic double layer near the sheet to the statistical properties of the hydration shells.

Index Terms—graphene nanopore, ion permeation, prehistory probability distribution, molecular dynamics

I. Introduction

Ionic transport through graphene nanopores is a rapidly expanding field encompassing both the nano- and biophysics communities. Being the smallest ion-selective devices, they find a wide range of applications including e.g. the desalination of water [1] and biosensing [2]. Analysis of permeation through them also sheds new light on the function of biological ion channels [3].

There are several issues that render prediction of the current in this system a challenging task, including: (i) formation of an ionic double layer near the graphene sheet, significantly altering the spatial distribution of ions in the bulk electrolyte [4]; (ii) the existence of fixed charge on the nanopore walls, modifying the structure of the double layer [5]; (iii) spatial dependence of the number [6] and orientation of water molecules in the hydration shells of the ions in the pore; (iv) dependence of the effective dielectric constant [7] ϵ_w and excess chemical potentials $\bar{\mu}_i$ of the ions [8] on their location within the pore; and (v) the position-dependent diffusivity [9] of ions in the proximity of the pore.

We note that each of the problems listed above is the subject of extensive independent research. The complexity of the system relates to the fact that the current through the pore, the statistics of the hydration shells, and the properties of the electrical double layer are mutually interrelated in a nontrivial manner, cf. [10]. These mutual interactions are often neglected to simplify the analysis,

e.g. the first hydration shell is often considered to be intact near a charged surface [5] even though it is known that dehydration and saturation of the water orientation have significant effects on the local [11] dielectric permittivity, the potential of the mean force [12], and, therefore, on the current through the pore.

In this work we provide atomistic insight into the interplay between dehydration, water polarization in the hydration shells, and the ionic double layer induced by the electrostatic field near the graphene surface. Statistical analysis is facilitated by introducing the prehistory probability distribution of ionic trajectories crossing the pore.

The paper is organized as follows. First, we introduce the model in Sec. II. Next, we discuss the structure of the electrical double layer (EDL), and discuss the prehistory density of the permeating ions, in Secs. III and Sec. IV respectively. The dehydration and water orientation in the first two shells of potassium ions crossing the pore are discussed in Sec. V. Finally, conclusions are drawn in Sec. VI.

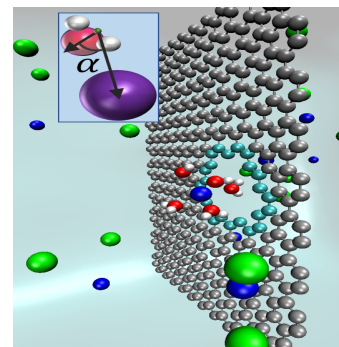


Fig. 1. VMD [13] image of the graphene nanopore surrounded by electrolyte solutions. Carbon atoms are shown in dark grey. Water molecules are explicitly resolved, but are shown here as a transparent glassy medium except for the 1st hydration shell of the K^+ ion (blue ball) crossing the pore. Chloride ions are shown in green. Charged carbon ions around the rim of the pore are shown in cyan. The orientation of one water molecule in the 1-st shell of the K^+ ion is illustrated in the inset.

[¶]Engineering and Physical Sciences Research Council (UK) Grant EP/M015831/1 and Leverhulme Trust Research Project Grant RPG-2017-134.

II. Model

The model considered is shown in Fig. 1. It consists of a single-layer graphene sheet separating two electrolyte solutions of one molar KCl on both sides. The pore through the middle of the graphene sheet has diameter $\sim 8\text{\AA}$ measured as the center-to-center separation of carbon atoms on opposite sides of the rim. Note that ionic radius of carbon atoms is 0.7\AA and the closest distance between K and Cl atoms is expected to be ≥ 240 pm (sum of van-der-Waals radii). So the actual radius of the pore seen by potassium ions is less than 3\AA as was confirmed by our simulations. Electric fields of either 0.006 or 0.01 $\text{V}/\text{\AA}$ (potential drops across the cell of 0.3 or 0.5 V) were applied in the direction normal to the graphene sheet. Two values of the fixed charge Q_f at the rim were considered: 0.75 and 2 (in units of the electron charge e).

The theory of the ion current through such nanopore can be formulated in terms of the density functional [14], [15]

$$F = \int dr \left[-\frac{\varepsilon_0 \varepsilon_r |\nabla \psi|^2}{2} + ez\psi(n_+ - n_-) - \mu_+ n_+ - \mu_- n_- - \mu_w n_w - Ts \right] \quad (1)$$

where ε_0 and ε_r are the vacuum and electrolyte permittivities, n_i ($i = +, -, w$) are the number densities of positive (K^+) and negative (Cl^-) ions and water molecules, μ_i ($i = +, -, w$) are the chemical potentials of ions and water molecules, T is the temperature and s is the entropy density, respectively. Here the local electrostatic potential ψ is found by solving Poisson's equation taking explicit account of the applied potential, the fixed charge on the pore rim, the ionic distribution in the EDL, and the orientation of the water molecules in the bulk electrolyte [5].

Close to the charged nanopore, ε_r and μ_i may each become a function of ionic position as well as of the EDL structure and the pore charge. One important mechanism of such coupling is the variation in the number and orientation of water molecules in the 1st and 2nd hydration shells of the permeating ion, in the presence of the EDL for nonzero Q_f . In turn, this variation affects the height of the potential barrier separating the left ($z > 0$) and right electrolytes [6], [12] which is what controls ion current through the pore.

To provide insight into this coupling we perform molecular dynamics (MD) simulations of the system in Fig. 1. The cell size of the model is $37 \times 37 \times 50$ \AA , the number of water molecules is 1871, and the number of ions of each type is 36. The simulation time was ~ 1 μs in each case, the time step was 1 fs, and the NPT ensemble was used in the NAMD package [16]. The atomic trajectories were saved every 1 ps.

III. Electrical double layer

As discussed in the introduction a key feature of this system is the formation of the ionic double layer near the

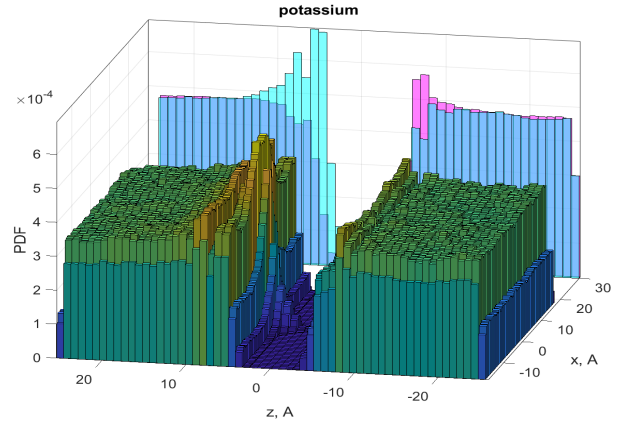


Fig. 2. Probability distribution of potassium ions in the ZY plane. The back plane shows a 1D PDF of K^+ (cyan) and Cl^- (pink) ions in the cylinder $x^2 + y^2 < R_2$, $|z| < 25\text{\AA}$.

graphene sheet, induced by the electric field and modified by the fixed charge of the pore. An example of the layers of potassium ions is shown in Fig. 2 for the case $Q_f = 0.75e$ and $\Delta V = 0.5$ V. The 2D PDF corresponds to the distribution of potassium ions in the layer $|y| \leq 8\text{\AA}$.

It can be seen from the figure that the layers have plane symmetry away from the charge pore. Near the pore the plane symmetry is broken and the concentration of K^+ ions has a well pronounced peak.

On the back plane of the figure the local structure of the EDL is shown as 1D distributions of the potassium and chloride ions in a cylinder aligned with the pore axis. The cylinder radius $R_2 \approx 6\text{\AA}$ corresponds to the outer radius of the 2nd hydration shell. It can be seen from the figure that the electrolyte solutions are charged on both sides near the pore. The charge in this case can be estimated as $\sim 0.26e$ for the left ($z > 0$) and $\sim -0.05e$ for the right-hand baths. The structure and charge of the EDL is adjusted self-consistently to the changes in applied voltage and fixed charge on the rim. We therefore conjecture that the number of water molecules and their orientation in the 1st and 2nd hydration shells of K^+ ion crossing the pore are affected by the EDL. The coupling between the EDL, the charge of the rim, and the structure of hydration shells is nontrivial.

IV. Prehistory probability distribution

To reveal this coupling we employ a method of analysis of the permeating ion trajectories based on the prehistory probability distribution function (PPDF) [17], [18] extended to non-equilibrium systems [19]. To build the PPDF we note that, for $Q_f \leq 2e$, crossing events are well-localized in time – it takes on average less than 1 ps for potassium ion to cross the plane of the graphene sheet at $z = 0\text{\AA}$. We also note that the crossings are sufficiently rare to be considered as independent events: the transition from the left ($z > 0$) to the right bath can be considered as rare escape events over a potential barrier

with the time interval between them ranging between ~ 14 ns ($Q_f = 0.75e$) and 0.4 ns ($Q_f = 2e$)

It therefore becomes possible to collect the escape trajectories of potassium ions and superimpose them using the moment of the ion's transition through the pore as a time marker. The result of such superposition for $Q_f = 2e$ is illustrated by plotting three superimposed escape trajectories at the top plane of Fig. 3. It can be seen from the figure that the transition events are indeed easily recognised sharp features of the trajectories that can be used for their efficient superposition.

To build the PPDF escape, trajectories were extended both backwards in time (hence the name "prehistory" PDF) and forwards (which for convenience we refer to as the "posthistory" PDF) from the marker by 200 ps. The resultant distribution of superimposed trajectories is shown in Fig. 3. The 1D distributions of the potassium and chloride ions in a cylinder aligned with the pore axis, shown here for $Q_f = 2e$ in the back plane, is similar to that shown in Fig. 2.

It can be seen from the figure that the local structure of the EDL has significantly changed its shape as compared to the case $Q_f = 0.75e$. We now observe two sharp peaks of potassium ions on both sides of the pore due to the strong negative charge of the pore rim. The charge of these layers is estimated as $\sim 0.42e$ for the left ($z > 0$) and $\sim 0.45e$ right baths correspondingly.

It can also be seen from the figure the PPDF has sharp peaks for permeation trajectories approaching and leaving the pore. These peaks indicate that K^+ ions accumulate and dwell (for ~ 100 ps) in the local EDL before and after escape event. This observation confirm the conjecture (see Sec. III) that the hydration shells of escaping ions can be affected by the structure of the EDL, as well as by the charge of the rim and the applied voltage. The details of

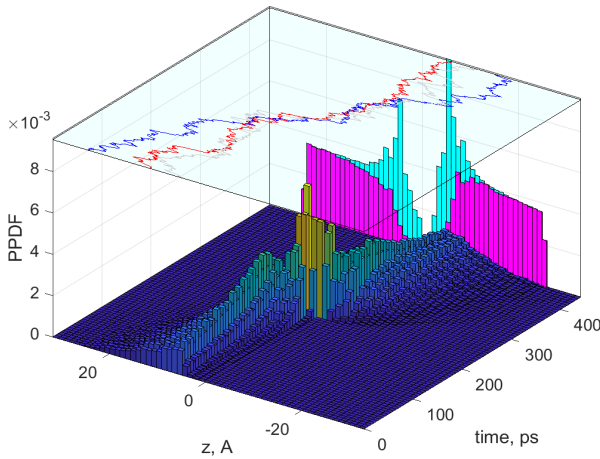


Fig. 3. The PPDF of ionic trajectories crossing the pore. Top plane: example of three escape trajectories superimposed using the permeation event as the time marker. Back plane: 1D PDF of K^+ (cyan) and Cl^- (pink) ions in a cylinder $x^2 + y^2 < R_2$, $|z| < 25\text{\AA}$

these correlations can now be quantified by analysing the measured prehistory probability distribution.

V. Dehydration and water polarization in the pore

To quantify these correlations we build the most probable escape path [17]–[19] by averaging the z -coordinate along the PPDF. These paths are shown in Fig. 4 by black solid and thin dashed lines for $Q_f = 2e$ and $0.75e$ respectively. The changes in the local structure of the EDL discussed above for $Q_f = 2e$ reveal themselves as the change in slope of the mean path immediately after a permeation event and the shift of the mean path towards the graphene sheet ($z = 0$). The properties of the hydration shells can now be analyzed along the mean path.

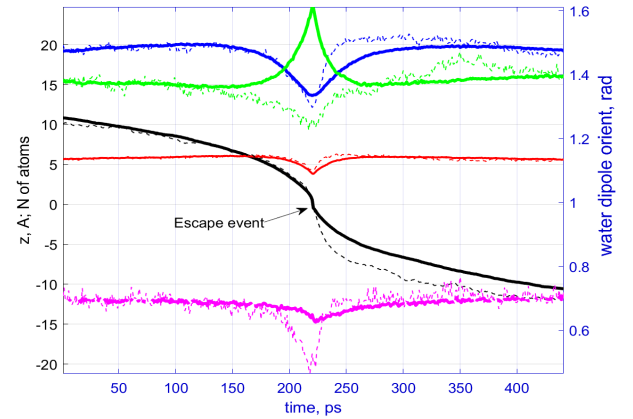


Fig. 4. Left y-axis: Mean values of the coordinate along the trajectories of ions crossing the pore (black lines). Number of ions in the 1st (red) and 2nd (blue) shells along the mean coordinate. Right y-axis: Mean values of orientation of the water dipole for the water molecules in the 1st (green) and 2nd (pink) shells. $Q_f = 2e$ - thick solid lines; $Q_f = 0.75e$ - thin dashed lines.

First, we notice that the numbers of water molecules in the 1st (N_1) and 2nd (N_2) hydration shells of K^+ ions (shown by red and blue lines respectively in the figure) alter during the transition, as compared to their bulk values. Thus N_2 is reduced from 20 (in the bulk) to ~ 12 (in the pore) for $Q_f = 0.75e$ and to ~ 14 for $Q_f = 2e$. Similarly, N_1 is reduced from 6 to ~ 3.8 in the pore for both values of Q_f . This dehydration plays a major role in formation of the potential barrier impeding permeation events, cf [6], [12]

The effect of the local EDL structure on the number of water molecules in the hydration shells is most clearly seen in the relaxation of these numbers back to their bulk values immediately after a transition event. For $Q_f = 0.75e$ the relaxation time is shorter than 50 ps for both shells. For $Q_f = 2e$ the relaxation time is increased to ~ 70 ps for the 1st shell and to ~ 160 ps for the 2nd shell.

Next, we note the changes in the orientation of water molecules in the 1st (α_1 , see Fig. 1) and the 2nd (α_2) hydration shells of K^+ ions (shown by magenta and green lines respectively in the figure) during the transition

events. Thus α_1 is reduced from 0.22 in (units of π) to 0.15 for $Q_f = 0.75e$. One would expect that the value of α_1 will be further reduced by increasing the Q_f from $0.75e$ to $2e$. However counter-intuitively, we observe that the value of α_1 in the pore is 0.2 and remains nearly the same as in the bulk. The relaxation time of α_1 towards its bulk value, after the transition event, is increased (cf. N_1 above), from 25 ps for $Q_f = 0.75e$, to ~ 70 ps.

The most significant EDL-induced changes are observed in the orientation of the water molecules in the 2nd shell. In the bulk, orientation of the water dipoles in this shell is almost tangential to the spherical surface passing through the water and centered at the ion with $\alpha_2 = 0.44$ (in π units). For $Q_f = 0.75e$ the dipoles within the pore turn slightly towards the ion crossing the pore $\alpha_2 = 0.4$. For $Q_f = 2e$, however the changes in the orientation are reversed and the dipoles turn away from the ion with $\alpha_2 = 0.51$. This flipping can be attributed to the fact the 2nd hydration shell extends all the way to the local EDL of potassium ions, and the accumulation of these ions near the pore forces the water dipoles to turn away from the ion in the pore.

VI. Conclusions

In conclusion, we have investigated the distribution of trajectories of potassium ions crossing a nano-pore in a single graphene sheet. We observed correlations between the number and orientation of water molecules in the 1st and 2nd hydration shells of these ions and the structure of the EDL formed near the pore, due to applied electrostatic potential and the charged rim of the pore.

In particular, it was found that the shape of the most probable escape trajectory and the relaxation time towards bulk values of the number of molecules in both shells, and of orientation of waters in the 1st shell, are significantly affected by the changes in the EDL induced by increasing the charge of the pore from $0.75e$ to $2e$. The same changes in the EDL structure force the orientation of the water dipoles in the 2nd hydration shell to flip from being oriented towards the pore center at $0.75e$ to orientation away from the pore center at $2e$.

The observed features shed a new light on the influence of the EDL on the spatial dependence of the excess chemical potential and the effective dielectric constant seen by ions transiting the pore, and will help in the development of self-consistent density functional theories of ion currents through nanopores.

Acknowledgment

We are grateful to Bob Eisenberg, Aneta Stefanovska, and the late Igor Kaufman for helpful discussions.

References

[1] Z. Li, Y. Qiu, K. Li, J. Sha, T. Li, and Y. Chen, "Optimal design of graphene nanopores for seawater desalination," *The Journal of Chemical Physics*, vol. 148, no. 1, p. 014703, jan 2018.

[2] M. Ali, B. Yameen, R. Neumann, W. Ensinger, W. Knoll, and O. Azzaroni, "Biosensing and supramolecular bioconjugation in single conical polymer nanochannels. facile incorporation of biorecognition elements into nanoconfined geometries," *Journal of the American Chemical Society*, vol. 130, no. 48, pp. 16351–16357, 2008, pMID: 19006302.

[3] B. Hille, *Ion Channels Of Excitable Membranes*, 3rd ed. Sunderland, MA: Sinauer Associates, 2001.

[4] D. Henderson, D. Gillespie, T. Nagy, and D. Boda, "Monte carlo simulation of the electric double layer: dielectric boundaries and the effects of induced charge," *Molecular Physics*, vol. 103, no. 21-23, pp. 2851–2861, nov 2005.

[5] E. Gongadze, L. Mesarec, V. Kralj-Iglic, and A. Iglic, "Asymmetric finite size of ions and orientational ordering of water in electric double layer theory within lattice model," *Mini-Reviews in Medicinal Chemistry*, vol. 18, no. 18, pp. 1559–1566, oct 2018.

[6] M. Zwolak, J. Lagerqvist, and M. Di Ventra, "Quantized ionic conductance in nanopores," *Phys. Rev. Lett.*, vol. 103, p. 128102, 2009.

[7] B. Eisenberg and W. Liu, "Relative dielectric constants and selectivity ratios in open ionic channels," *Computational and Mathematical Biophysics*, vol. 5, no. 1, oct 2017.

[8] Y. Zhou and R. MacKinnon, "The occupancy of ions in the K^+ selectivity filter: Charge balance and coupling of ion binding to a protein conformational change underlie high conduction rates," *J. Mole. Biol.*, vol. 333, no. 5, pp. 965–975, 2003.

[9] J. Comer, C. Chipot, and F. D. González-Nilo, "Calculating position-dependent diffusivity in biased molecular dynamics simulations," *Journal of Chemical Theory and Computation*, vol. 9, no. 2, pp. 876–882, jan 2013.

[10] S. Sahu and M. Zwolak, "Maxwell-hall access resistance in graphene nanopores," *Physical Chemistry Chemical Physics*, vol. 20, no. 7, pp. 4646–4651, 2018.

[11] E. Gongadze, A. Velikonja, Š. Perutkova, P. Kramar, A. Maček-Lebar, V. Kralj-Iglič, and A. Iglič, "Ions and water molecules in an electrolyte solution in contact with charged and dipolar surfaces," *Electrochimica Acta*, vol. 126, pp. 42–60, apr 2014.

[12] W. A. T. Gibby, M. L. Barabash, C. Guardiani, D. G. Luchinsky, and P. V. E. McClintock, "The role of noise in determining selective ionic conduction through nano-pores," in *2018 IEEE 13th Nanotechnology Materials and Devices Conference (NMDC)*, Oct 2018, pp. 1–6.

[13] W. Humphrey, A. Dalke, and K. Schulten, "VMD: Visual molecular dynamics," *Journal of Molecular Graphics*, vol. 14, no. 1, pp. 33–38, feb 1996.

[14] J.-S. Sin, Y.-M. Jang, C.-H. Kim, and H.-C. Kim, "Steric effect of water molecule clusters on electrostatic interaction and electroosmotic transport in aqueous electrolytes: A mean-field approach," *AIP Advances*, vol. 8, no. 10, p. 105222, oct 2018.

[15] D. G. Luchinsky, W. A. T. Gibby, I. Kaufman, D. A. Timucin, and P. V. E. McClintock, "Statistical theory of selectivity and conductivity in biological channels," *arXiv preprint arXiv:1604.05758*, 2016.

[16] J. C. Phillips, R. Braun, W. Wang, J. Gumbart, E. Tajkhorshid, E. Villa, C. Chipot, R. D. Skeel, L. Kalé, and K. Schulten, "Scalable molecular dynamics with NAMD," *Journal of Computational Chemistry*, vol. 26, no. 16, pp. 1781–1802, 2005.

[17] M. I. Dykman, P. V. E. McClintock, V. N. Smelyanskiy, N. D. Stein, and N. G. Stocks, "Optimal paths and the prehistory problem for large fluctuations in noise driven systems," *Phys. Rev. Lett.*, vol. 68, no. 18, pp. 2718–2721, 1992.

[18] D. G. Luchinsky and P. V. E. McClintock, "Irreversibility of classical fluctuations studied in analogue electrical circuits," *Nature*, vol. 389, no. 6650, pp. 463–466, 1997.

[19] I. A. Khovanov, D. G. Luchinsky, P. V. E. McClintock, and A. N. Silchenko, "Fluctuational escape from chaotic attractors in multistable systems," *International Journal Of Bifurcation And Chaos*, vol. 18, no. 06, pp. 1727–1739, jun 2008.